JCHR (2020) 10(4), 287-296

Journal of Chemical Health Risks

www.jchr.org

ORIGINAL ARTICLE

Plasmonic Nanosilver Synthesis Using *Sonneratia apetala* Fruit Extract and Their Catalytic Activity in Organic Dye Degradation

Muhammad Shamim Al Mamun*, Md Israil Hossain, Jannatul Naime, Palash Kumar Dhar

Chemistry Discipline, Khulna University, Khulna-9208, Bangladesh

(Received: 1 July 2020 Accepted: 5 September 2020)

KEYWORDS

Nanosilver;
Green synthesis;
Surface plasmon;
Resonance;
Catalytic activity;
Degradation;
Sonneratia apetala

ABSTRACT: Comparing to the chemical and physical techniques, biosynthesis of nanoparticles is being facilitated due to its nontoxic and economically feasible availability. In this present study, plant-mediated silver nanoparticles (AgNPs) were synthesized using the fruit extract of *Sonneratia apetala* from the silver nitrate ($AgNO_3$) solution. Among different physiological conditions, effect of reaction time was investigated during the AgNPs synthesis. Surface Plasmon Resonance (SPR) characterization was conducted for verifying the nanoparticles size and morphology. A distinct band centered around 400-480 nm in the UV-Visible spectroscopy represented the formation of AgNPs. FTIR spectroscopy revealed that –OH group may play important role for the reduction of Ag^+ to AgNPs. XRD revels the face-centered cubic geometry of AgNPs. AFM image analysis helped to find out the shape of the synthesized AgNPs is sphereical. The efficiency of AgNPs as a promising catalyst through electron transfer in the degradation of methyl orange and methyl red was investigated. This catalytic activity of AgNPs can be used to synthesis different chemical intermediates and organic transformations.

INTRODUCTION

Nowadays, research in the field of nanotechnology has been flourished to overcome environmental and technological demanding in the area of medicine, wastewater treatment and energy conversion [1]. Instead of using external chemicals responsible for the environmental contamination bio-route mediated synthesis of several metallic nanoparticles are of promising interest to the researchers [2]. Green route synthesis has been developed due to its non-toxic, cost effective and economical concern. In the last few decades, nanomaterials synthesis is of great attraction because of their unique sensing, catalytic activity, drug delivery, electrical and optical phenomena [3-5].

Among metallic nanoparticles, silver nanoparticle (AgNP) dominants its place in nanomaterials due to its exclusive characteristics attainable in various fields. Due to the appreciable antimicrobial activity and anticancer agents AgNPs are being synthesized by many researchers [6]. The pristine silver can be served as the highest electrical and thermal conductivity amidst all the metals [7]. The behavior of nanoparticles varies according to their shape,

*Corresponding author: s.mamun@ku.ac.bd (M. Sh. Al Mamun)
DOI: 10.22034/jchr.2020.1904366.1155

size and morphology [8]. Different functions derive from the fact that nanoscale ranges exhibit distinct properties as compared to their bulk counterpart because of their huge surface to volume ratio [9]. Many researchers have been reported about the environment friendly reducing and capping agents for the nanomaterials synthesis [10, 11]. Synthesis of silver nanoparticles (AgNPs) by the different parts of the plants have been reported [12-14]. Several microorganisms such as fungi, yeasts, bacteria [15] and nuclear materials like DNA [16] have also been scrutinized for the AgNPs synthesis. There is an important and unique optical property exhibited by all the metal nanoparticles named surface plasmon resonance (SPR). SPR can be used as a fingerprint for the identification of the formation of metal nanoparticle [9].

Organic dyes have been used in the industries such as food, leather, cosmetic, paper, textile, plastic and pharmaceutical industries for a prolonged period of time [17-19]. These effluents ensue drastic environmental contamination. Especially, azo dyes were distinguished as probable carcinogens [20, 21]. Discharged dyes are highly resistant to microorganisms so the reduction through the biological methods are fruitless [22]. Thus, the evolution of simple method for the significant degradation of dyes has boosted greater interest [23]. Because of the large surface to volume ratios, metal nanoparticles exhibit significant catalytic activity for the degradation of dyes.

Biomolecules present in the fruit extract of *Sonneratia apetala* are mostly polyphenols and have good antioxidants properties [24]. *Sonneratia apetala* fruit extract can be used as a protection from acetaminophen induced liver injury in mice [25]. Although the medicinal properties of *Sonneratia apetala* fruit extract has been revealed but the reducing capacity has not been tested.

The present research reports the synthesis of AgNPs using the fruit extract of *Sonneratia apetala* as a reducing agent. The SPR phenomena of the AgNPs was evaluated for the nanoparticle formation, size estimation and their optical band gap determination. FTIR was used to confirm the functionals groups of the phytochemicals responsible for the reduction of $AgNO_3$ to AgNPs. X-Ray Diffraction (XRD) was taken to confirm the crystallinity of the synthesized Ag nanoparticles. Catalytic properties of synthesized Ag nanoparticles were examined for the degradation of organic dye using $NaBH_4$ and monitored by UV-Visible spectrophotometer. Successful degradation of organic dyes using Ag nanoparticles indicate the functionality of the synthesized AgNPs as a catalyst.

MATERIALS AND METHODS

Materials

Silver nitrate ($AgNO_3$), sodium borohydride ($NaBH_4$), MO and MR were purchased from sigma Aldrich and were used without further purification. The fruit of *Sonneratia apetala* (see supporting information) was collected freshly from Khulna district, Bangladesh. The fruit was thoroughly washed with deionized distilled water and then it was cut into smaller pieces and preserved.

Preparation of plant extract

About 20 g of finely cut fruits were kept in a round bottom flask containing 100 mL deionized distilled water and boiled for 20 min. the extract was cooled down and filtered with filter paper (What Mann no: 42) and stored at 4°C for further use.

Synthetic procedure for AgNPs

The process of synthesis was followed from the following research work[26] but with a simple modification. Prior to the experiment, all the glass wares were cleaned thoroughly by the distilled water to abstain residual chemical contamination. 100 mL 2 mM $AgNO_3$ solution was prepared in a volumetric flask and this flask covered with carbon paper to prevent autoxidation of silver. 2.0 mL of aqueous fruit extract of *Sonneratia apetala* was taken in a conical flask. Then 40.0 mL of freshly prepared 2 mM $AgNO_3$ was added into the conical flask. The aqueous extract and $AgNO_3$ were mixed and heated on oil bath at 60°C for 30 min with constant stirring until the color change was observed. The color change of reaction mixture from colorless to reddish brown indicate the formation of silver nanoparticles by *Sonneratia apetala* fruit extract.

Preparation of colloidal AgNPs

The reaction mixture containing AgNPs were centrifuged at 13,000 rpm for 30 min and the precipitate was thoroughly washed with sterile distilled water for three times to get rid of any unwanted impurities. Then total volume was converted into 10 mL. This is colloidal solution. This solution was used as a catalyst in organic dyes degradation and AFM analysis. The purified pellet was then dried at 60°C and then the sample was characterized by Fourier Transform Infra-Red (FTIR) using KBr pellet.

Catalytic Degradation of Organic Dyes

1 mL 100mM Sodium borohydride ($NaBH_4$) and 1mL 10^{-3}M Methyl orange or Methyl Red was taken in a beaker. The solution was made up to 10 mL by adding with distilled water. 1 mL colloidal AgNP solution was used to see the effect of AgNPs as a catalyst.

Characterization technique

UV-Visible Spectroscopy

The formation of silver nanoparticles in the medium was confirmed by the surface plasmon resonance band (SPR) observed by UV-Vis absorption spectroscopy (Model: LABOMED, INC, UVD-3200 PC).

FTIR Spectroscopy

The functional groups available in the compounds of fruit extract of *Sonneratia apetala* was studied by the FTIR spectrometer (model: SHIMADZO FTIR-4200). Characterization was carried out in the rage of 500 cm^{-1} to 4000 cm^{-1} using KBr pellet.

Atomic Force Microscope (AFM)

AFM image was collected from XE-100-TTK (Park systems, Inc.) scanning probe microscope in noncontact mode. The topographic images were recorded at a force constant of 42 N/m and resonant frequency of 354 kHz. The area of scanning was 1 μm^2 with a scan rate of 0.5 Hz.

RESULTS AND DISCUSSION

Effect of physiological condition on AgNPs formation

The size, shape and the morphology of the AgNPs are affected by the different physiological and environmental conditions such as time, extract concentration. After mixing the fruit extract of *Sonneratia apetala* with the $AgNO_3$ solution, the color change from colorless to reddish brown confirms the formation of AgNPs into the solution (see supporting information). Different types of biomolecules present in the extract of *Sonneratia apetala* are responsible for the reduction of silver ions to AgNPs [27]. After a certain time, there was no further color change of the mixed solution indicated the total reduction of Ag ions. The strong surface plasmon resonance was exhibited by the AgNPs in the solution [28]. Metal nanoparticles interacting with the lights cause collective oscillation of the conductive electrons on the metal surface know as surface plasmon resonance (SPR). This SPR is unique property for the metal nanoparticles. Because of the special optical feature of AgNPs, an extreme deal of information can be achieved from the UV-Vis spectra. Peak of the plasmon resonance shifts to longer wavelength and widens when the particle diameter enlarges [22]. Band wavelength, width and the effect of secondary resonances can be used as a spectral fingerprint for the plasmonic nanoparticles with a unique shape and size. The secondary band may cause due to the quadruple resonance that has a different electron oscillation pattern than the primary dipole resonance [22]. The silver nanoparticles using plant extract emits light within the range of 300-700 nm depending on the size, shape and the morphology [29]. The absorption peak intensity increased after 440 nm may be due to the increasing of formation of AgNPs with the increase of extract amount and reaction time.

The size of the AgNPs was calculated by the following equation (1)[30]:

$$d = \frac{h v_f}{\pi \Delta E_{1/2}} \qquad (1)$$

Where d is the diameter of the particle, h is the Planck's constant, v_f is the Fermi velocity of electron is the bulk silver and $\Delta E_{1/2}$ is the full width at half maximum (FWHM) of the absorption band. This equation is valid as long as the size of the AgNPs is less than the mean free path of the electrons in bulk silver [31].

The optical band gap of the synthesized AgNPs was calculated using the following equation (2) [32]:

$$E = \frac{hc}{\lambda_{max}} \qquad (2)$$

Where, h is the Planck's constant, v is the velocity of light and λ_{max} is the maximum absorbance edge.

The reaction time had an important effect on the formation of AgNPs. In Figure 1, as the reaction time was increased an increment of absorbance obtained with the passage of time indicating the enhancement in the formation of AgNPs. With the increase of time the absorbance increased but the full width half maximum (FWHM) decreased signified the increased of the particle sizes while the decrease of the band gap of the synthesized AgNPs [33]. The estimated particle size varied from around 14 nm to 21 nm since the time period was extended from 30 min to 90 min (calculated from equation 1). The band gap was found to be changed from 1.73 eV to 1.68 eV when the time was increased from 30 min to 90 min. There is an inverse correlation between the band gap and the particle size. Band gap increases while the particle size decreases because the electron hole pairs are now much closer together and the Coulombic interaction between them can no longer be neglected giving an overall higher kinetic energy [34].

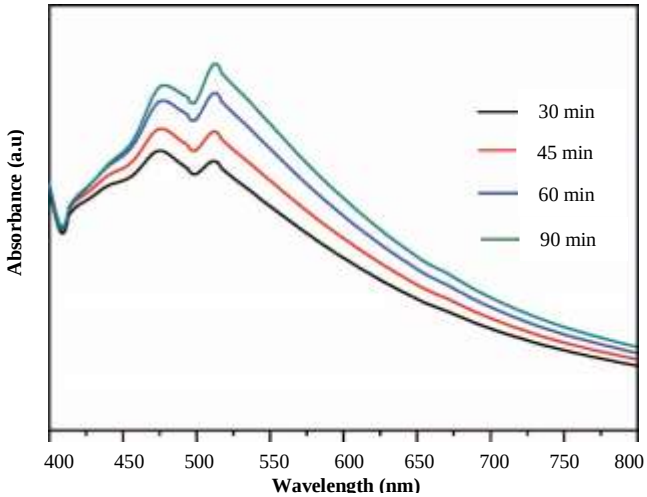

Figure 1. Absorbance spectra of AgNPs using fruit extract of *Sonneratia apetala* with variation of reaction time.

FTIR analysis

Biomolecules present in the *Sonneratia apetala* fruit extract plays an important role for the reduction and stabilization of the facile synthesized AgNPs. Possible functional groups from the biomolecules can be assumed from the FTIR spectroscopy (shown in Figure 2). The broad band peak found at 3421 cm^{-1} may be due to the stretching vibrations of –OH group in the *Sonneratia apetala* fruit extract. Peak at 3056 cm^{-1} could be for the aromatic C-H vibration[35]. Peak around 1362 cm^{-1} would be for the $–CH_2$- and $-CH_3$ bend stretching. Peak observed at 1580 cm^{-1} is due to the stretching vibrational peak of Ar-C=C-H[35]. Another peak at 830 cm^{-1} could be due to the 1,4-substituted aromatic ring [35]. FTIR study revealed that phenolic group present in the biomolecules have the great affinity for the nanoparticles and participate for the formation of the AgNPs [22].

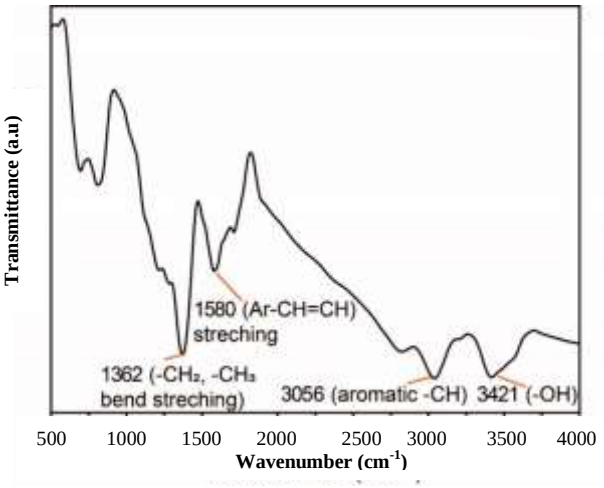

Figure 2. FTIR spectra of *Sonneratia apetala* fruit extract.

XRD analysis

The X-ray diffraction pattern clearly shows the formation of face centered cubic crystalline silver nanoparticles shown in Figure 3. The diffraction pattern shows the peaks at two theta values of 38.05, 44.51 and 64.95 with lattice plane (111), (200) and (220), respectively[36]. The diffraction peaks well matched with the standard data files (JCPDS card no. 04–0783) confirming the formation of Ag-NPs. AgNPs size was calculated using XRD data according to the Debye-Scherrer method and found 12.29 nm, which is compatible with the calculation from the optical measurement.

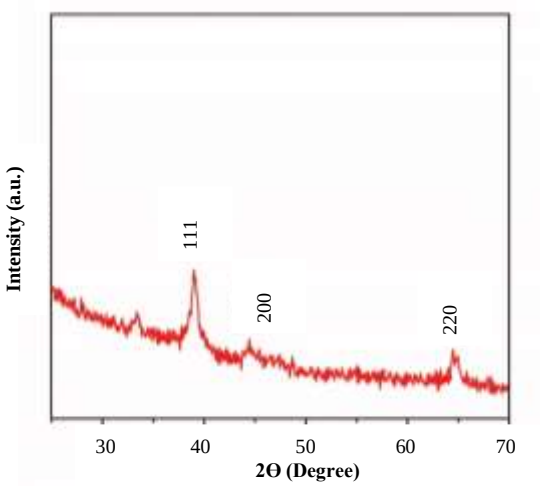

Figure 3. XRD pattern of the synthesized Ag nanoparticles.

Atomic Force Microscope analysis

The particle shape, size and the morphology can be attributed from the AFM image (Figure 4). AFM was measured using SiO_2/MoS_2 as a substrate. At first image was taken for the only substrate (Figure 4a). After that substrate was dipped into the colloidal AgNPs for 30 sec and then measured the AFM image. From figure 4b, the AgNPs are seen on the substrate surface. From Figure 4 it is seen that particles are mostly spherical[37].

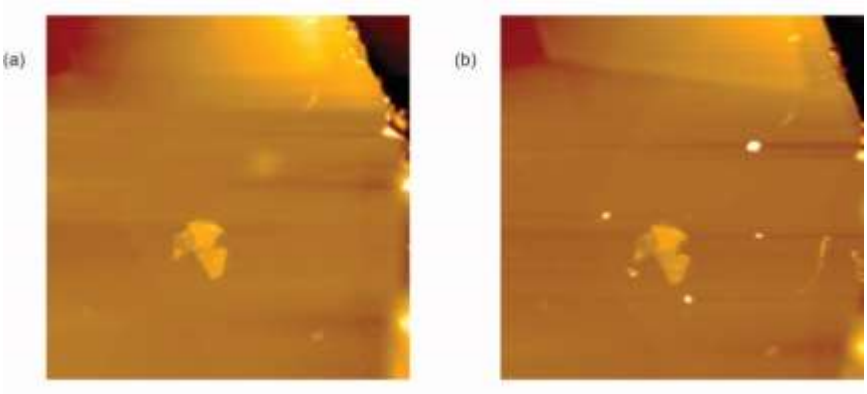

Figure 4. AFM image of the MoS_2 substrate (a) before (pristine) and (b) after AgNPs incorporation.

Catalytic degradation of methyl orange and methyl red

Because of the extreme use of the dyes in the industries, several stable and toxic dyes are very much harmful for the environment, thus it is imperious to manage environmental safety for human being. Methyl orange, an organic sulfosalt, reduction by the $NaBH_4$ was carried out (0 min to 20 min) without AgNPs (shown in Figure 5a), but there is no visible reduction observed or the rate was very slow which comply with the reported work [22, 38].

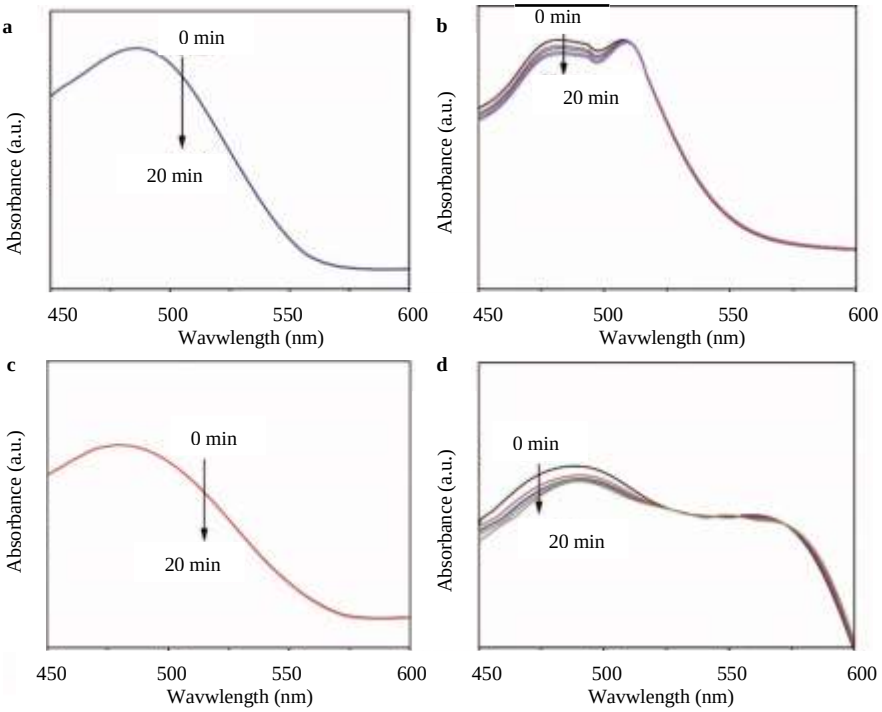

Figure 5. Degradation of methyl orange and methyl red to its corresponding products by $NaBH_4$ a) MO in absence of AgNPs and b) MO in presence of AgNPs (c) MR in absence of AgNPs (d) MR in presence of AgNPs.

Metal nanoparticles can be used as a catalyst for the reduction of dyes due to their high reactive activity and specific surface area. Figure 5b shows the reduction of MO by the $NaBH_4$ in presence of AgNPs. The absorbance band of MO arises at 480 nm in the absorbance spectra. After addition of silver nanoparticles into the MO and $NaBH_4$ solution, adsorption take place between the well dispersed AgNPs and the MO molecules. The redox reaction occurred between the active MO and the $NaBH_4$ more easily because of the effective surface adsorption of AgNPs on the MO molecules hence the absorbance spectrum showed the decreasing peaks in intensity for MO dye at different time period (0 min to 20 min), which is compatible with the previous report[22]. The color of the solution before and after degradation of MO is shown in supporting information. The degradation mechanism can be shown in the following mechanism[22]:

$Ag/NaBH_4 + h\nu \longrightarrow Ag/NaBH_4 (h^+\text{-}e^-)$

$2e^- + MOH^+ + H^+ \longrightarrow MOH_2^-$ (hydrazine derivative)

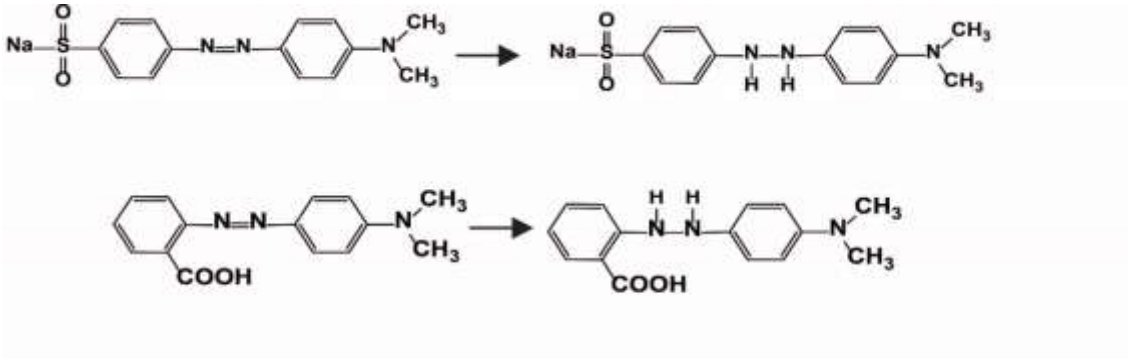

Degradation rate of MR was examined by the $NaBH_4$ (0 min to 20 min) in absence of produced AgNPs shown in figure 5c. From this figure, it is confirmed that there is no change of absorbance intensity of MR with the $NaBH_4$ or the degradation rate was so slow. While AgNPs were added to the MR and $NaBH_4$ solution, the absorbance intensity was decreased with the time intervals (0 min to 20 min) shown in figure 5d, which comply with the reported work[38]. The initial color of methyl red solution totally changed after addition of AgNPs, shown in supporting information. From the absorbance spectrum (5b & 5d), it is seen that MO and MR are not completely degraded. This is may be due to the inadequate electron release from the nanoparticles thus slower the dye degradation or the amount of AgNPs were not sufficient up to complete dye degradation. May be irradiation of photon on the AgNPs can enhance the catalytic activity of AgNPs[39].

Kinetic study was conducted for the calculation of the rate constants for the degradation of methyl orange and the methyl red. Ln (A/A_0) vs time plot was plotted for both cases of methyl orange and methyl red. Upon data analysis, the result emphasized that the degradation of dye appears to follow the first order kinetics (Figure 6a & 6b). The rate constants for the methyl orange and the methyl red were 0.044 min^{-1} and 0.01 min^{-1} respectively.

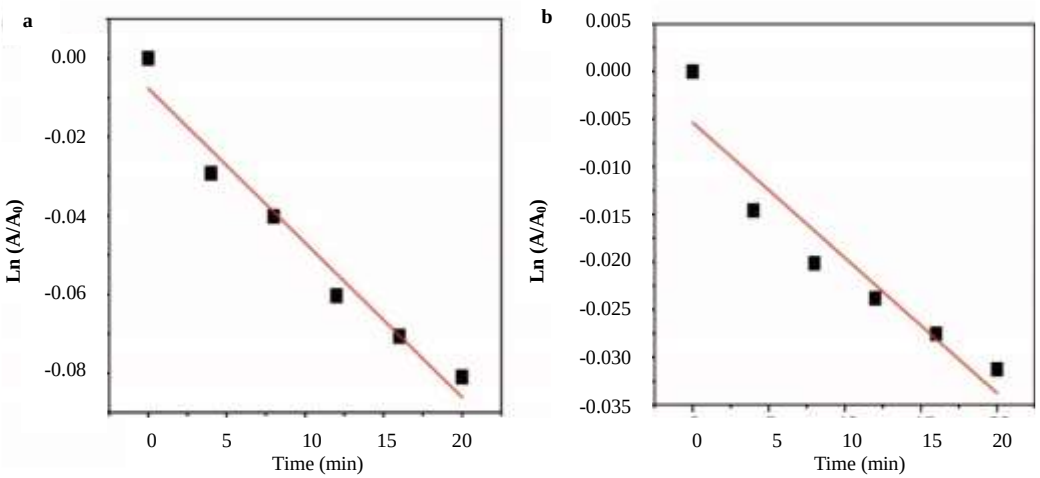

Figure 6. a) Ln (A/A_0) vs time plot of methyl orange b) Ln (A/A_0) vs time plot for methyl red.

CONCLUSIONS

A cost-effective, non-toxic facile synthesis of AgNPs was demonstrated through the reduction of $AgNO_3$ (aq) solution using fruit extract of *Sonneratia apetala*. Surface plasmon resonance was considered as a unique characteristic of the AgNPs confirmation and their optical band gap calculation. FTIR revealed the functional groups present in the extract can play significant role for the reduction of Ag^+ to AgNPs and AFM measurement signifies the shape of the formed AgNPs. XRD pattern confirmed the formation of crystalline AgNPs. The use of AgNPs as a catalyst was investigated in the case of methyl orange and methyl red degradation in the presence of $NaBH_4$. This catalytic activity of AgNPs can be used to synthesis different chemical intermediates and organic transformations. Effect of photon on the dye degradation may faster the degradation using AgNPs synthesized using *Sonneratia apetala* fruit extract.

CONFLICT OF INTEREST

The authors declare that there has no conflict of interest.

REFERENCES

1. Salata O., 2004. Applications of nanoparticles in biology and medicine. J Nanobiotechnology. 2(1), 1-6.

2. Amin M., Anwar F., Janjua M.R.S.A., Iqbal M.A., Rashid U., 2012. Green Synthesis of Silver Nanoparticles through Reduction with *Solanum xanthocarpum* L. Berry Extract: Characterization, Antimicrobial and Urease Inhibitory Activities against Helicobacter pylori. International Journal of Molecular Sciences. 13(8), 9923-9941.

3. Mehata M.S., Majumder M., Mallik B., Ohta N., 2010. External Electric Field Effects on Optical Property and Excitation Dynamics of Capped CdS Quantum Dots Embedded in a Polymer Film. Journal of Physical Chemistry C. 114(37), 15594-15601.

4. Mehata M.S., 2015. Enhancement of Charge Transfer and Quenching of Photoluminescence of Capped CdS Quantum Dots. Scientific Reports. 5, 12056.

5. Velmurugan P., Shim J., Bang K.S., Oh B.T., 2016. Gold nanoparticles mediated coloring of fabrics and leather for antibacterial activity. Journal of Photochemistry and Photobiology B-Biology. 160, 102-109.

6. AshaRani P.V., Mun G.L.K., Hande M.P., Valiyaveettil S., 2009. Cytotoxicity and Genotoxicity of Silver Nanoparticles in Human Cells. Acs Nano. 3(2), 279-290.

7. Seiler H.G., Sigel H., 1988. Handbook on toxicity of inorganic compounds. Marcel Dekker. United States.

8. Khlebtsov N.G., Trachuk L.A., Mel'nikov A.G., 2005. The effect of the size, shape, and structure of metal nanoparticles on the dependence of their optical properties on the refractive index of a disperse medium. Optics and Spectroscopy. 98(1), 77-83.

9. Mehata M.S., Mehata M.S., 2017. Medicinal Plant Leaf Extract and Pure Flavonoid Mediated Green Synthesis of Silver Nanoparticles and their Enhanced Antibacterial Property. Scientific Reports. 7,15867.

10. Tavakoli F., Salavati-Niasari M., Ghanbari D., Saberyan K., Hosseinpour-Mashkani S.M., 2014. Application of glucose as a green capping agent and reductant to fabricate CuI micro/nanostructures. Materials Research Bulletin. 49, 14-20.

11. Gholami T., Salavati-Niasari M., Varshoy S., 2016. Investigation of the electrochemical hydrogen storage and photocatalytic properties of CoAl2O4 pigment: Green synthesis and characterization. International Journal of Hydrogen Energy. 41(22), 9418-9426.

12. Arya A., Gupta K., Chundawat T.S., Vaya D., 2018. Biogenic Synthesis of Copper and Silver Nanoparticles Using Green Alga Botryococcus braunii and Its Antimicrobial Activity. Bioinorganic Chemistry and Applications.

13. Ibrahim H.M.M., 2015. Green synthesis and characterization of silver nanoparticles using banana peel extract and their antimicrobial activity against representative microorganisms. Journal of Radiation Research and Applied Sciences. 8(3), 265-275.

14. Reddy N.J., Vali D.N., Rani M., Rani S.S., 2014. Evaluation of antioxidant, antibacterial and cytotoxic effects of green synthesized silver nanoparticles by Piper longum fruit. Materials Science & Engineering C-Materials for Biological Applications. 34, 115-122.

15. Narayanan K.B., Sakthivel N., 2010. Biological synthesis of metal nanoparticles by microbes. Advances in Colloid and Interface Science. 156(1-2), 1-13.

16. Sohn J.S., Kwon Y.W., Jin J.I., Jo B.W., 2011. DNA-Templated Preparation of Gold Nanoparticles. Molecules. 16(10), 8143-8151.

17. Hameed B.H., Ahmad A.L., Latiff K.N.A., 2007. Adsorption of basic dye (methylene blue) onto activated carbon prepared from rattan sawdust. Dyes and Pigments. 75(1), 143-149.

18. Wanyonyi W.C., Onyari J.M., Shiundu P.M., 2014. Adsorption of Congo Red Dye from Aqueous Solutions Using Roots of Eichhornia crassipes: Kinetic and Equilibrium Studies. Technologies and Materials for Renewable Energy. Environment and Sustainability (Tmrees14 - Eumisd). 50, 862-869.

19. Khellaf N., Djelal H., Amrane A., Cabrol A., 2018. Biostimulation to improve the dye biodegradation of organic dyes by activated sludge. Journal of Chemical Health Risks. 7(4), 247-258.

20. Chung K.T., Cerniglia C.E., 1992. Mutagenicity of azo dyes: structure-activity relationships. Mutat Res. 277(3), 201-220.

21. Kusic H., Koprivanac N., Srsan L., 2006. Azo dye degradation using Fenton type processes assisted by UV irradiation: A kinetic study. Journal of Photochemistry and Photobiology a-Chemistry. 181(2-3), 195-202.

22. Vidhu V.K., Philip D., 2014. Catalytic degradation of organic dyes using biosynthesized silver nanoparticles. Micron. 56, 54-62.

23. Mirzaie M., Rashidi A., Tayebi H.A., Yazdanshenas M.E., 2018. Preparation of SBA-15-PAMAM as a Nano Adsorbent for Removal of Acid Red 266 from Aqueous Media: Batch Adsorption and Equilibrium Studies. Journal of Chemical Health Risks. 7(4), 285-298.

24. Hossain S.J., Islam M.R., Pervin T., Iftekharuzzaman M., Hamdi O.A.A., Mubassara S., Saifuzzaman M., Shilpi J.A., 2017. Antibacterial, Anti-Diarrhoeal, Analgesic, Cytotoxic Activities, and GC-MS Profiling of Sonneratia apetala (Buch.-Ham.) Seed. Prev Nutr Food Sci. 22(3), 157-165.

25. Liu J., Luo D., Wu Y., Gao C., Lin G., Chen J., Wu X., Zhang Q., Cai J., Su Z., 2019. The Protective Effect of Sonneratia apetala Fruit Extract on Acetaminophen-Induced Liver Injury in Mice. Evid Based Complement Alternat Med. 2019, 6919834.

26. Khodashenas B., Ghorbani H.R., 2019. Synthesis of silver nanoparticles with different shapes. Arabian Journal of Chemistry. 12 (8), 1823-1838.

27. Ahumada M., Suuronen E.J., Alarcon E.I. 2019. Biomolecule Silver Nanoparticle-Based Materials for Biomedical Applications. In: L. M. T. Martínez, O. V. Kharissova and B. I. Kharisov (eds.) Handbook of Ecomaterials. pp. 3485-3501. Cham: Springer International Publishing.

28. Shankar S.S., Rai A., Ahmad A., Sastry M., 2004. Rapid synthesis of Au, Ag, and bimetallic Au core-Ag shell nanoparticles using Neem (Azadirachta indica) leaf broth. J Colloid Interface Sci. 275 (2), 496-502.

29. Vigneshwaran N., Ashtaputre N.M., Varadarajan P.V., Nachane R.P., Paralikar K.M., Balasubramanya R.H., 2007. Biological synthesis of silver nanoparticles using the fungus Aspergillus flavus. Materials Letters, 61(6), 1413-1418.

30. Rozra J., Saini I., Sharma A., Chandak N., Aggarwal S., Dhiman R., Sharma P.K., 2012. Cu nanoparticles induced structural, optical and electrical modification in PVA. Materials Chemistry and Physics. 134(2-3), 1121-1126.

31. Karthikeyan B., 2008. Fluorescent glass embedded silver nanoclusters: An optical study. Journal of Applied Physics. 103. 114313, 1-5.

32. Gharibshahi L., Saion E., Gharibshahi E., Shaari A.H., Matori K.A., 2017. Structural and Optical Properties of Ag Nanoparticles Synthesized by Thermal Treatment Method. Materials. 10(4), 402.

33. Avinash B.S., Chaturmukha V.S., Jayanna H.S., Naveen C.S., Rajeeva M.P., Harish B.M., Suresh S., Lamani A.R., 2016. Effect of Particle Size on Band Gap and DC Electrical Conductivity of TiO_2 Nanomaterial. International Conference on Condensed Matter and Applied Physics (Icc 2015). 1728. 020426,1-4.

34. Ferreira D.L., Sousa J.C. L., Maronesi R.N., Bettini J., Schiavon M.A., Teixeira A.V.N.C., Silva A.G., 2017. Size-dependent bandgap and particle size distribution of colloidal semiconductor nanocrystals. Journal of Chemical Physics. 147(15), 154102,1-9.

35. Nikolic G., Zlatkovic S., Cakic M., Cakic S., Lacnjevac C., Rajic Z., 2010. Fast Fourier Transform IR Characterization of Epoxy GY Systems Crosslinked with Aliphatic and Cycloaliphatic EH Polyamine Adducts. Sensors. 10(1), 684-696.

36. Singh R., Sahu S.K., Thangaraj M., 2014. Biosynthesis of Silver Nanoparticles by Marine Invertebrate (Polychaete) and Assessment of Its Efficacy against Human Pathogens. Journal of Nanoparticles. 1-7.

37. Hamedi S., Shojaosadati S.A., 2019. Rapid and green synthesis of silver nanoparticles using Diospyros lotus extract: Evaluation of their biological and catalytic activities. Polyhedron. 171, 172-180.

38. Ganapuram B.R., Alle M., Dadigala R., Dasari A., Maragoni V., Guttena V., 2015. Catalytic reduction of methylene blue and Congo red dyes using green synthesized gold nanoparticles capped by salmalia malabarica gum. International Nano Letters. 5(4), 215-222.

39. Vijayalakshmi S., Elaiyappillai E., Johnson P.M., Lydia I.S., 2020. Multifunctional magnetic $CoFe_2O_4$ nanoparticles for the photocatalytic discoloration of aqueous methyl violet dye and energy storage applications. Journal of Materials Science: Materials in Electronics. 31(13), 10738-10749.